

See discussions, stats, and author profiles for this publication at: <https://www.researchgate.net/publication/236327194>

Fluorescent Ru(phen)₃(²⁺)-Doped Silica Nanoparticles-Based ICTS Sensor for Quantitative Detection of Enrofloxacin Residues in Chicken Meat

ARTICLE in ANALYTICAL CHEMISTRY · APRIL 2013

Impact Factor: 5.64 · DOI: 10.1021/ac400502v · Source: PubMed

CITATIONS

15

READS

157

7 AUTHORS, INCLUDING:



Xiaolin Huang

Nanchang University

11 PUBLICATIONS 52 CITATIONS

SEE PROFILE



Zoraida P Aguilar

Zystein, LLC

87 PUBLICATIONS 796 CITATIONS

SEE PROFILE



Hengyi Xu

Nanchang University

77 PUBLICATIONS 623 CITATIONS

SEE PROFILE

Fluorescent Ru(phen)₃²⁺-Doped Silica Nanoparticles-Based ICTS Sensor for Quantitative Detection of Enrofloxacin Residues in Chicken Meat

Xiaolin Huang,^{†,‡,§} Zoraida P. Aguilar,^{§,§} Huaiming Li,[‡] Weihua Lai,[†] Hua Wei,^{†,‡} Hengyi Xu,^{*,†} and Yonghua Xiong^{*,†,‡}

[†]State Key Laboratory of Food Science and Technology, Nanchang University, Nanchang 330047, P. R. China

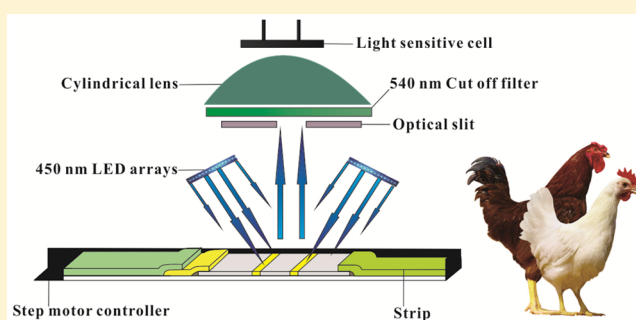
[‡]Jiangxi-OAI Joint Research Institute, Nanchang University, Nanchang 330047, P. R. China

[§]Zystein, LLC., Fayetteville, Arkansas 72704, U.S.A.

S Supporting Information

ABSTRACT: A Ru(phen)₃²⁺-doped silica fluorescent nanoparticle (FN)-based immunochromatographic test strip (ICTS) sensor was developed for rapid, high sensitivity, easy to use, and low cost quantitative detection of enrofloxacin (ENR) residues in chicken meat. The fluorescence signal intensity of the FNs at the test line (FI_T) and control line (FI_C) was determined with a prototype of a portable fluorescent strip reader. Unique properties of Ru(phen)₃²⁺ doped silica nanoparticles (e.g., large Stokes shift, high emission quantum yield, and long fluorescence lifetime) were combined with the advantages of ICTS and an easy to make portable fluorescent strip reader. The signal was based

on FI_T/FI_C ratio to effectively eliminate strip to strip variation and matrix effects. Various parameters that influenced the strip were investigated and optimized. Quantitative ENR detection with the FNs ICTS sensor using 80 μL sample took only 20 min, which is faster than the commercial ELISA kit (that took 90 min). The linear range of detection in chicken extract was established at 0.025–3.500 ng/mL with a half maximal inhibitory concentration at 0.22 ± 0.02 ng/mL. Using the optimized parameters, the limit of detection (LOD) for ENR using the FNs ICTS sensor was recorded at 0.02 ng/mL in chicken extract. This corresponds to 0.12 μg/kg chicken meat which is two (2) orders of magnitude better than the maximum residue limits (MRLs) imposed in Japan (10 μg/kg) and three (3) orders of magnitude better than those imposed in China. The intra- and inter-assay coefficient of variations (CVs) were 6.04% and 12.96% at 0.5 ng/mL, 6.92% and 12.61% at 1.0 ng/mL, and 6.66% and 11.88% at 2.0 ng/mL in chicken extract, respectively. The recoveries using the new FNs ICTS sensor from fifty (50) ENR-spiked chicken samples showed a highly significant correlation ($R^2 = 0.9693$) with the commercial enzyme-linked immunosorbent assay (ELISA) kit. The new FNs ICTS sensor is a simple, rapid, sensitive, accurate, and inexpensive quantitative detection of ENR residues in chicken meat and extracts.



Food safety monitoring for chemical contamination has become necessary because of the presence of chemicals that can harm consumers.^{1–5} Among the current methods used to detect the presence of harmful chemicals with high selectivity and sensitivity, immunosensors with electrochemical or optical transducers have been widely studied and proposed.^{6–9} Among the immunosensors, immunochromatographic strip sensors have been used in monitoring veterinary residuals, mycotoxin pollution, as well as for pathogen detection. Compared with traditional gold nanoparticles that are used in immunochromatographic test strip (ICTS) sensors, fluorescent labels including organic dyes,¹⁰ up-converting phosphorus,^{11–13} quantum dots,^{14,15} and europium chelate doped nanoparticles^{16,17} have attracted much attention because of advantages that include sensitivity, ease of use, rapidity,

quantification, and portability making these suitable for on-site trace-level detection in food and food-related materials.¹⁸

Ruthenium(II) complexes such as Ru(phen)₃²⁺, as transition-metal-based luminophore, have potential applications as reporter labels in biosensors because of large Stokes shift, high emission quantum yield and long fluorescence lifetime.¹⁹ However, its relative low fluorescence intensity and poor photochemical stability result in low sensitivity. Encapsulation inside silica nanoparticles protect thousands of the inorganic ruthenium(II) from oxidation damage.^{20,21} In general, the inorganic ruthenium(II) is premixed with TEOS solution at the beginning of the reaction, which causes aggregation of the

Received: February 11, 2013

Accepted: April 25, 2013

Published: April 25, 2013

ruthenium(II) in the core of the silica nanoparticles that result in reduced fluorescence efficiency due to fluorescence self-quenching.²² Improved synthesis led to a few examples of ruthenium(II) complex doped silica nanoparticles with improved fluorescence intensity and stability for ultrasensitive detection of biomolecules.^{20,21}

In this paper, an improved method for the synthesis of Ru(phen)₃²⁺-doped silica nanoparticles was carried out by delaying the addition time of Ru(phen)₃²⁺ in the reaction mixture. The delay suppressed the aggregation of the Ru(phen)₃²⁺ molecules during the condensation reaction, which led to enhanced fluorescence emission intensity.²² The highly fluorescent Ru(phen)₃²⁺-doped silica nanoparticles were used as a reporter for the strip sensor in the ultrasensitive quantitative detection of ENR residues in chicken meat.

As one of the most-often used fluoroquinolones (FQs), enrofloxacin (ENR) exhibits a broad spectrum of antibacterial properties, and is used exclusively in livestock for protection against veterinary diseases and as a growth-promoting pharmaceutical.^{23–25} However, ENR residues in animal meat and tissues may have potential risks to bacterial resistance causing detrimental changes in animal intestinal microbiota and may lead to anaphylactic reactions.^{24,26–28} Consequently, a number of countries in various regions have set up corresponding regulations to supervise the use of ENR in livestock and poultry. The European Commission and the Ministry of Agriculture of China have set up the same maximum residue limits (MRLs) for ENR and its active metabolite (ciprofloxacin) in animal muscle tissues at 100 µg/kg (MOA Bulletins 2002 No. 235). Japan has established lower MRLs in all chicken tissues (10 µg/kg, Ministry of Health and Welfare 2005) while the Food and Drug Administration of United States prohibits the use of ENR in poultry entirely.²⁷

Our group has previously described a colloidal gold-based chromatographic strip sensor for qualitative screening of ENR residue.²⁵ The cutoff detection was 3 ng/mL in phosphate-buffered saline (PBS) and 8 µg/kg in chicken meat.²⁵ Zhao et al reported a strip reader for colloidal gold immunochromatographic strip sensor that was used for quantitative determination of ENR residues in chicken meat with a linear range from 0.038 to 22.75 ng/mL and a half maximal inhibitory concentration (IC₅₀) at 0.935 ng/mL.²⁹ However, the results are not reliable because quantification was based only on the optical density of gold nanoparticles that were captured on the test lines. Signal variation from strip to strip, immunoreaction time, and the effect of sample matrices including variations in pH and ionic strength, all of which can influence the immunoreaction efficiency between the antibody and antigen, thereby, causing inaccurate quantification in real sample testing were not evaluated. Thus, in the present study, we report the development of a FNs ICTS sensor for ENR based on the ratio between the FI_T (fluorescence intensity at the test line) and FI_C (fluorescence intensity at the control line), FI_T/FI_C, signal ratio to normalize the signal and eliminate the effect of the above-mentioned parameters.

In the present work, we have developed a Ru(phen)₃²⁺-doped silica nanoparticles based immunochromatographic strip sensor, the FNs ICTS sensor, for quantitative detection of low concentrations of ENR. A portable reader was developed for possible on-site detection of ENR residues in chicken meat and meat extracts. The standard linear regression equation was determined and stored in the software that was built into the device called the “watchdog”. The “watchdog” was interfaced

with the fluorescent strip reader to store, normalize, and analyze the raw data. The performance of the FNs ICTS sensor was evaluated on raw chicken meat samples with respect to the limit of detection (LOD), the IC₅₀ value, accuracy, and precision. The new FNs ICTS sensor was compared with a commercially available ELISA kit to verify the sensitivity and reliability in fifty (50) raw chicken meat samples.

MATERIALS AND METHODS

Materials and Instruments. Enrofloxacin (ENR), bovine serum albumin (BSA), and *N*-(3-dimethylaminopropyl)-*N'*-ethylcarbodiimide hydrochloride (EDC·HCl) were purchased from Sigma-Aldrich Chemical Co. (St. Louis, MO). Sample pad, conjugate release pad, nitrocellulose membrane, and absorbent pad were obtained from Schleicher and Schuell GmbH (Dassel, Germany). Donkey antimouse IgG was purchased from Beijing Zhongshan Biotechnology, Inc. (Beijing, China). ENR-BSA conjugates and anti-ENR monoclonal antibodies (anti-ENR mAbs) were prepared and characterized in our laboratory as described previously.²⁵ The commercialized ELISA kit for ENR was obtained from Jiangxi Zodolabs Biotech. Corp. (Jiangxi, China). Phosphate buffer (PB, 0.02 M) was prepared by adding 20.06 g of Na₂HPO₄·12H₂O and 5.92 g of NaH₂PO₄·2H₂O in 1000 mL of Milli-Q water and adjusted to pH 7.0 (unless otherwise specified) before use. Other reagents were of analytical grade and purchased from Sinopharm Chemical Corp. (Shanghai, China).

The BioDot XYZ platform combined with a motion controller, BioJet Quanti3000k dispenser and AirJet Quanti3000k dispenser for solution dispensing was supplied by BioDot (Irvine, CA). The vacuum drying oven was purchased from Shanghai Sumsung Laboratory Instrument Co., Ltd. (Shanghai, China). An automatic programmable cutter was purchased from Shanghai Jinbiao Biotechnology Co., Ltd. (Shanghai, China). Ultrapure water was prepared by Elix-3 and Milli-QA (Molsheim, France). Ru(phen)₃²⁺-doped silica nanoparticles were prepared and characterized as described in the Supporting Information.

2.2. Optimization of the Anti-ENR mAbs Conjugation to FNs Forming FNs-mAbs. To determine the optimum amount of the mAbs for the preparation of the FNs-mAbs, different volumes (10, 15, and 20 µL) of anti-ENR mAbs (2.0 mg/mL) were added to 1 mg of FNs in the presence of 7.5 µg EDC·HCl with 2 mL of 0.02 M PB buffer, pH 5.0. After reaction at room temperature for 2 h on a magnetic stirrer, the mixture was blocked with 200 µL of 10% BSA (w/v) for 30 min. The unreacted mAbs and anti-ENR mAbs conjugates (FNs-mAbs) were separated by centrifugation at 8000 rpm for 5 min and then the precipitates were washed with 2 mL of 0.02 M PB buffer, pH 5.0. The FNs-mAbs were resuspended in 200 µL solution containing 0.02 M Na₂HPO₄, 5% sucrose (w/v), 3% trehalose (w/v), 0.1% NaN₃, and 0.05% PEG 20000. The fluorescence intensities and average hydrodynamic diameters of the FNs and FNs-mAbs (0.5 mg/mL) were determined by Hitachi F-4500 fluorescence spectrophotometer (Tokyo, Japan) and particle size analyzer (Malvern Instruments Ltd., Worcestershire, U.K.), respectively.

Additionally, the extent of conjugation was qualitatively tested using Fourier transform infrared spectroscopy (FTIR Nicolet5700, Thermo Fisher Scientific, Inc., U.S.A.). Free anti-ENR mAbs (1.825 mg/mL), FNs (0.5 mg/mL), and FNs-mAbs (0.5 mg/mL) were individually ground with spectroscopic-grade potassium bromide before they were placed in the

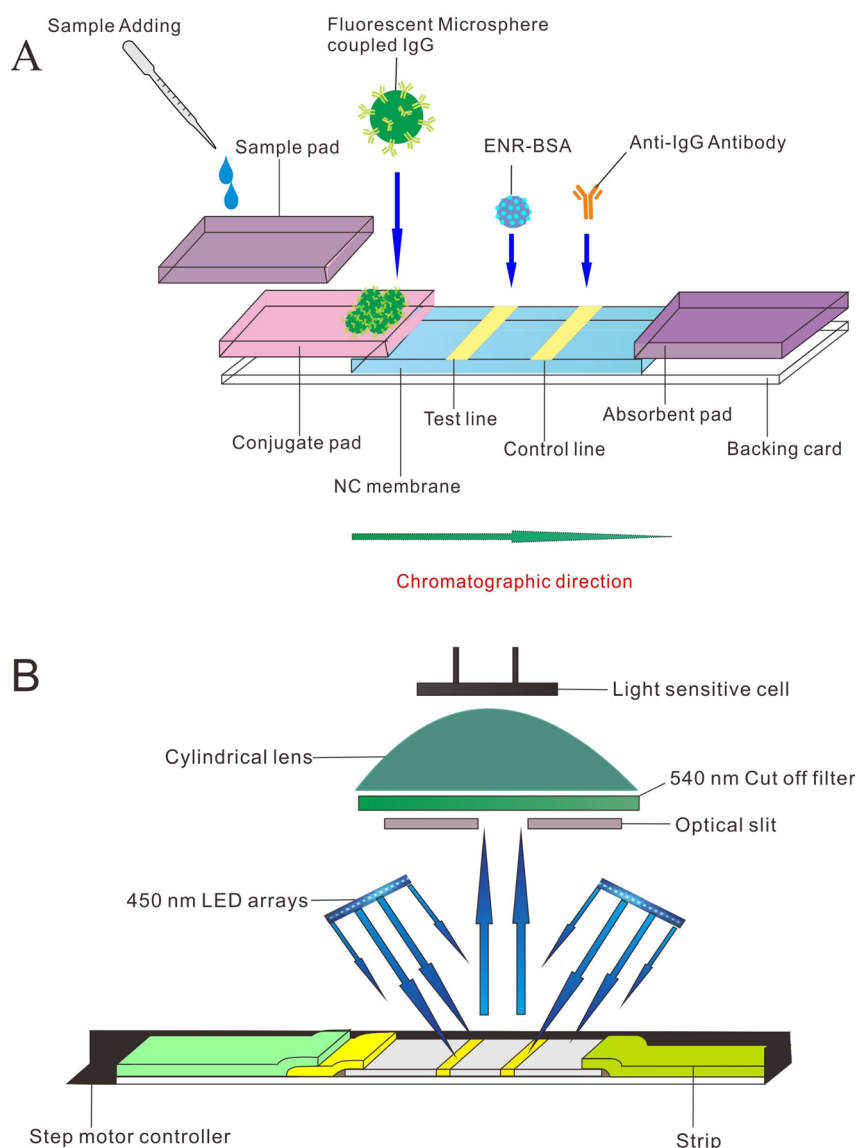


Figure 1. Schematic of the FNs strip fabrication (A) and diagram of the fluorescence strip reader (B).

sample cell respectively, and the diffuse reflectance spectra were scanned over 500–4000 cm^{-1} .

Fabrication of FNs ICTS Sensor. The schematic of FNs ICTS sensor fabrication is shown in Figure 1A. The strip consisted of four parts: sample pad, conjugate pad, nitrocellulose membrane (NC), and absorbent pad. The sample pad was saturated with a 50 mM Tris-HCl buffer (pH 8.0) containing 0.5% (w/v) PVP-10, 0.5% (v/v) Tween-20, 0.5% casein, and 0.02% NaN_3 . This was dried at 60 °C for 2 h. The conjugate pad was pretreated with a 50 mM Tris-HCl buffer (pH 8.0), including 0.5% (v/v) Tween-20, 5% sucrose, and 0.02% NaN_3 , and was dried at 37 °C for 12 h.

The signal was optimized with respect to the FNs-mAbs by spraying a 5 mg/mL concentration using a dispenser with a 1 mm diameter tip onto 30 cm \times 1 cm piece of conjugate pad material at 3, 4, or 5 $\mu\text{L}/\text{cm}$, respectively, and then dried with a vacuum dryer at 37 °C for 2 h. The FNs-mAbs treated conjugate pads were eventually cut into 4 mm \times 1 mm pieces.

To determine the amount of ENR-BSA needed to generate the optimum signal for the sensor, different concentrations of ENR-BSA antigen (1.0, 1.5, and 2.0 mg/mL, respectively) at

0.3 μL were dispensed at the test line on the NC membrane. At the control line, excess amount of the antibody against the FNs-mAbs, donkey-antimouse antibody (Abs, 1.0 mg/mL) were dispensed. The NC membrane was dried at 37 °C for 12 h before it was blocked with a 0.01 M PBS buffer containing 3% BSA (w/v) and 0.1% Tween-20 for 3 min. After they were washed with a 0.01 M PBS buffer containing 0.1% Tween-20 for three times, the blocked NC membranes were dried at 37 °C for 2 h. Finally, the strip was assembled by attaching the NC membrane, conjugate pad, sample pad, and absorbent pad that were overlapped 2 mm on top of each other onto the backing card. The assembled ICTS were cut into 4 mm wide sensor strips using an automatic programmable cutter. The sensor strips were packaged in a plastic bag containing a desiccant gel and stored at room temperature until use.

Overview of the Competitive Type FNs ICTS Sensor and Strip Reader. A competitive immunoassay for ENR was developed on the FNs ICTS sensor. When chicken liquid extracts containing ENR were added to the sample well, the ENR molecules migrated into the conjugate pad and bound with the FNs-mAbs to form FNs-mAbs–ENR complex that

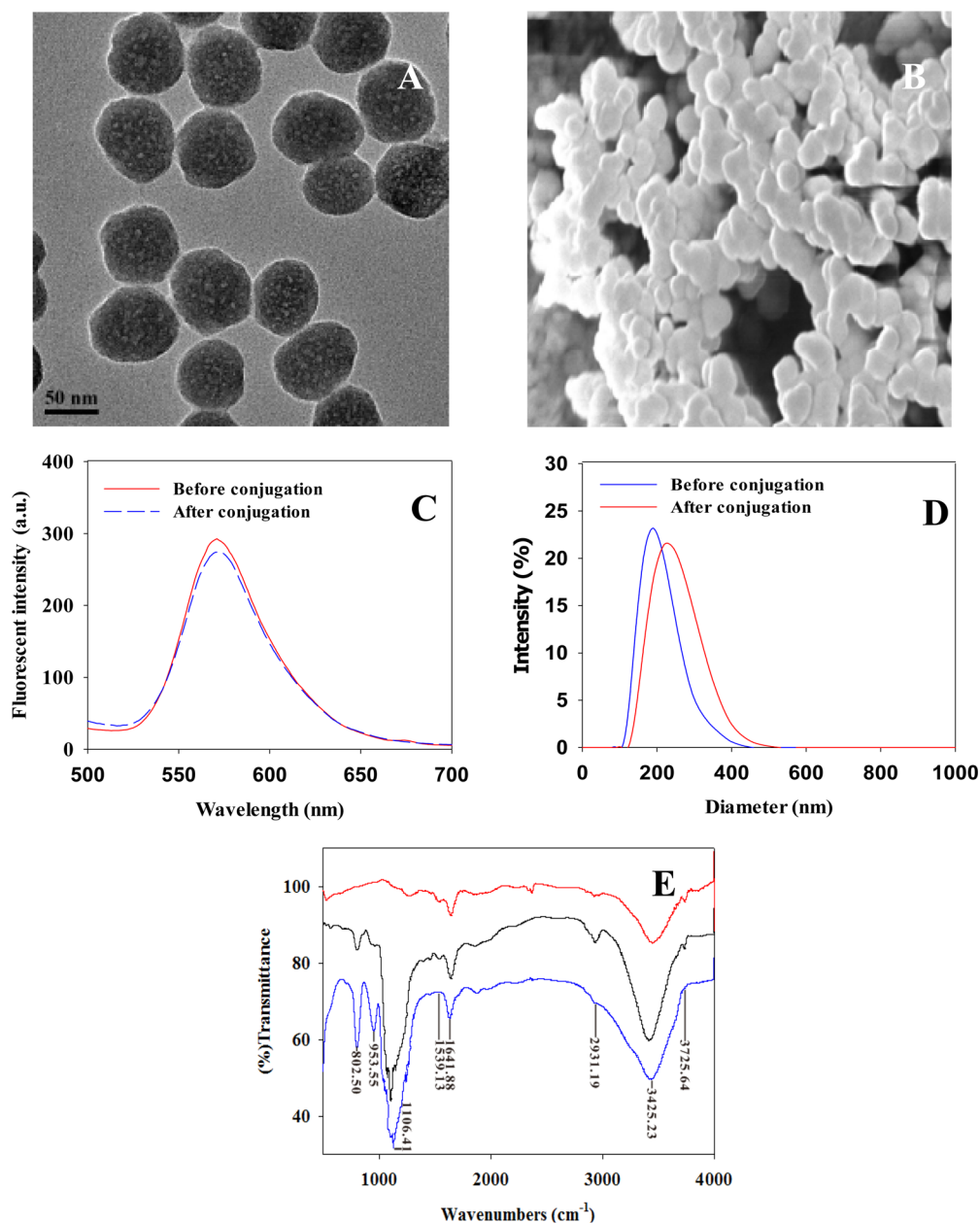


Figure 2. Characterization of the free FNs and FNs-mAbs conjugates. Transmission electron microscope image of FNs (A), scanning electron microscope image (B), fluorescence intensity of FNs before/after conjugation with antibody (0.5 mg/mL) (C), and hydrodynamic diameter of FNs before/after conjugation with antibody (0.5 mg/mL) (D) and FTIR spectra of mAbs (top), FNs (bottom), and FNs-mAbs (middle) (E).

migrated across the NC membrane and lodged on the Abs on the control line which resulted in the fluorescent signal. Unbound FNs-mAbs were attached to the ENR-BSA and lodged at the test line. The higher the amount of ENR in the sample, the lower the fluorescence intensity at the test line because of the competition between the ENR and the ENR-BSA.

In order to record the values of FI_T , FI_C , and FI_T/FI_C ratio, a portable fluorescence strip reader was assembled and interfaced with the “watchdog” that recorded the data and calculated the ENR concentration in the sample. The design of the reader is shown in Figure 1B. A step motor controller was used to transport the strip into the reader. A high power 450 nm LED arrays was used as excitation light source. The blue light produced by the 450 nm LED eliminated with a 540 nm cut off filter. The emission fluorescence of the FNs on the test and

control lines were focused with a cylindrical lens and received by a light sensitive cell after passing through an optical slit. The captured ENR concentration was calculated against a standard that has been incorporated into the software that was built into the “watchdog”.

Spiked Raw Chicken Meat Samples. The blank raw chicken samples, which were ascertained to be ENR free by LC/MS/MS, were bought from the surrounding food markets. Only the lean meat was cut into small pieces, frozen, and stored at $-20\text{ }^{\circ}\text{C}$ before use. Fifty (50) independent blank chicken samples (1 g for each sample) were prepared. The ENR stock solution (100 ng/mL in 0.01 M PB, pH 7.0) was added to each of these meat samples using 3.75–202.5 μL to a final concentration of 0.375–20.25 $\mu\text{g}/\text{kg}$. Each sample was stored at $4\text{ }^{\circ}\text{C}$ for 24 h and then extracted for ENR detection with the new FNs ICTS sensor and the commercial ELISA kit.

Chicken meat extracts were prepared as described previously with some modifications.²⁵ In brief, 1.0 g of chicken meat was homogenized and incubated at 80 °C for 5 min, then mixed with 3 mL of 0.01 M PB, pH 7 containing 0.6 M NaCl for 3 min with vigorous shaking. After centrifugation at 4000g for 5 min, the residue was re-extracted with the same procedures. The two supernatant solutions with a total volume of 6 mL were combined and used for analysis.

Three ENR-free chicken meat extracts were spiked with ENR at concentration of 0.5, 1.0, and 2.0 ng/mL for precision analysis. Note that the dilution factor between the extract (ng/mL) and real samples ($\mu\text{g/kg}$) was 6-fold, therefore, 1 ng/mL chicken extract = 1 kg chicken meat containing 6 μg of ENR.

Optimization of the Quantitative FNs ICTS Sensor Parameters. Various parameters were optimized including salt concentration, sample pH, and the most effective reaction time by analyzing the kinetics of the FNs ICTS immunosensor. To determine the most appropriate pH value, 0.01 M PB buffer with 0.6 M NaCl at a pH of 4–9 were evaluated. Salt solutions of 0.01 M PB buffer (pH 7) containing 0, 0.1, 0.2, 0.4, 0.5, 0.6, and 0.7 M NaCl, were prepared to obtain the best ionic strength for the sensor. Each of these solutions was used to prepare 1.0 ng/mL ENR for the assay optimization.

The optimum detection time at the above conditions was established. An 80 μL of the ENR at the various conditions was placed in the sample well. After 1 min, the strip was inserted in the strip reader and readings were recorded every 30 s for a total of 40 min. Both the FI_T and the FI_C were recorded. The kinetics of the reaction was determined by plotting the FI_T and FI_C individually against time.

Generation of Standard Calibration Curve. Using the optimized conditions (pH 7.0, 0.6 M NaCl, 1.0 mg/mL ENR-BSA, FNs-mAbs (prepared with 30 μg of mAbs labeled with 1 mg FNs, 5 mg/mL) that was dispensed at 3 $\mu\text{L/cm}$), the standard calibration curve was generated by running twelve standard ENR spiked ENR-free chicken meat extracts to final concentrations of 0 (as negative control), 0.025, 0.05, 0.1, 0.2, 0.4, 0.6, 0.8, 1.0, 2.0, 3.0, and 3.5 ng/mL, respectively. The ratio of the $\text{FI}_\text{T}/\text{FI}_\text{C}$ of negative control and positive standard samples were designated B_0 (stands for $\text{FI}_\text{T}/\text{FI}_\text{C}$ of negative control) and B (stands for $\text{FI}_\text{T}/\text{FI}_\text{C}$ of positive samples), respectively. The standard curve was constructed by plotting the inhibition rate (B/B_0) ratios against the logarithm of the ENR concentrations. The value of B_0 and the linear regression equation were built into the “watchdog” software.

Comparative Evaluation with Commercial ELISA Kit for ENR. Fifty (50) raw chicken meat samples were spiked with ENR from 0.375 (0.0625 ng/mL) to 20.25 $\mu\text{g/kg}$ (3.375 ng/mL) to evaluate the real sample application of the FNs ICTS sensor. To evaluate the reliability and sensitivity of the new FNs ICTS sensor, the same samples were also analyzed with a commercial ENR ELISA kit.

Statistical Analysis. Statistical significance was determined by analysis of variance (ANOVA) followed by F test. A $P < 0.05$ was considered statistically significant.

RESULTS AND DISCUSSION

Characterization of FNs and FNs-mAbs. In the present study, $\text{Ru}(\text{phen})_3^{2+}$ was doped into silica nanoparticles $\text{Ru}(\text{phen})_3^{2+}$ to improve the fluorescence intensity. The resulting FNs exhibited about 23,000 times higher luminescence intensity compared with $\text{Ru}(\text{phen})_3^{2+}$ alone (detailed calculation can be found in the Supporting Information). A thin

layer of polystyrene and poly(acrylic acid) was further polymerized on the surface of the $\text{Ru}(\text{phen})_3^{2+}$ -doped silica nanoparticles to reduce the response to changes in environmental factors, such as oxygen levels, pH, and ionic solution. The results can be found in the Supporting Information Figure S-1A and 1B. This polymer coating made the FNs surface more smooth which also decreased unwanted nonspecific binding.

Transmission and scanning electron microscope images of the FNs shown in Figure 2A and 2B indicated that the FNs appeared relatively regular in shape with good monodispersity and uniform size distribution with an average diameter of 77 ± 6 nm.

The FNs-mAbs were prepared by coupling the carboxyl group of the FNs with the amino group of anti-ENR mAbs using the active ester method as previously described.³⁰ A fluorescence spectrophotometer and particle size analyzer were used to characterize the FNs-mAbs and FNs. The fluorescence intensities of FNs-mAbs exhibited a slight weakening (6% decrease in signal) while the maximum emission wavelength did not shift compared with the free FNs (Figure 2C). This was presumably because the antibody on the surface of the nanoparticles shielded the fluorescence signal. Dynamic light scattering (DLS) analysis of the FNs showed that the average hydrodynamic diameter was not affected by pH or salt concentration (Supporting Information Figure S-3A and 3B) when the pH of the colloidal dispersion was changed from 5 to 9 and when the NaCl concentrations were 0.1 to 1.0 M. These results indicated that $\text{Ru}(\text{phen})_3^{2+}$ -doped silica nanoparticles were stable at pH 5 to 9 and in the presence of 0.1–1 M NaCl. On the other hand, DLS analysis of the FNs-mAbs showed that the average hydrodynamic diameter slightly increased from 202 to 226 nm (shown in Figure 2D).

To confirm that anti-ENR mAbs were immobilized on the surface of FNs, FTIR analysis was compared between the FNs alone, mAbs alone and the FNs-mAbs. As shown in Figure 2E, all three exhibited a peak at 3425.23, which corresponded to the COO-H that are found in the FNs alone, mAbs alone, and the FNs-mAbs.³¹ The FTIR spectra of mAbs and FNs-mAbs showed peptide bond characteristic peaks at 1641.88 ($\text{C}=\text{O}$ amide I) and 1539.19 cm^{-1} ($\text{N}-\text{C}=\text{O}$ amide II), whereas the FNs alone showed the $\text{C}=\text{O}$ stretch because of the poly(acrylic acid) coating, but it did not show the amide II bond signal. The FTIR peaks that were recorded for FNs-mAbs and the mAbs alone at 2931.19 cm^{-1} correspond to N–H stretch which was not found in FNs alone. The weak peak at 3725.64 cm^{-1} signal corresponding to O–H in amino acids were found on the FNs-mAbs and the mAbs but not on the FNs. The presence of the amide (from the peptides in the mAbs) linkages ($\text{C}=\text{O}$ and $\text{N}-\text{C}=\text{O}$), and the N–H and O–H on the FNs-mAbs demonstrated that the mAbs were successfully conjugated with the FNs.

Optimization of the FNs Strip Parameters. In the competitive immunoassay, the amount of antibody labeled with FNs, the dispensation rate ($\mu\text{L/cm}$) of the FNs-mAbs, and the concentration of ENR-BSA on the test line were a few of the parameters that controlled the limit of detection and the sensitivity of the strip, thus an orthogonal $\text{L}_9(3)^3$ test was designed for optimization. The results of orthogonal test and variant analysis indicated that the optimal combinations were as follows: 1.0 mg/mL ENR-BSA, 30 μg of mAbs labeled with 1 mg of free FNs, and 3 $\mu\text{L/cm}$ dispensation rate of FNs-mAbs. Under these conditions, the mean of FI_T and FI_C were 1287 ± 36 and 667 ± 26 ($n = 3$), respectively. The inhibition rate, that

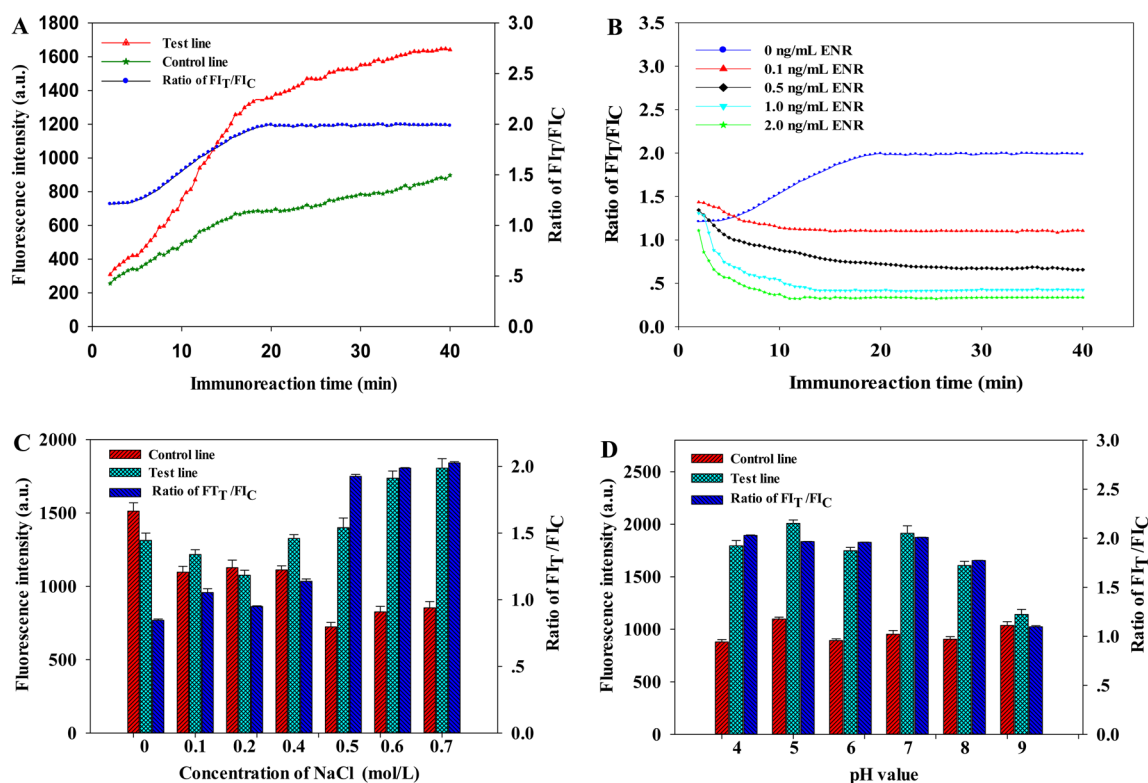


Figure 3. Optimization of various assay parameters. Immunoreaction kinetic curves of test line, control line, and ratio of FI_T/FI_C after addition of the blank (0.01 M PB buffer, pH 7.0) (A), immunoreaction kinetic curves of ratio of FI_T/FI_C after addition of 0.01 M PB buffer (pH 7) spiked with ENR at concentration of 0, 0.1, 0.5, 1.0, and 2.0 ng/mL (B), effects of different concentrations of NaCl (0, 0.1, 0.2, 0.4, 0.5, 0.6, 0.7 M) on the FI_T , FI_C , and the ratio of FI_T/FI_C (C), and different pH (4, 5, 6, 7, 8, 9) (D).

is defined as inhibition rate (%) = $B/B_0 \times 100$, where B_0 corresponds to the FI_T/FI_C of the negative control and B corresponds to FI_T/FI_C of the positive samples that were determined during the generation of the calibration curve, for the 1 ng/mL ENR concentration was $45.7\% \pm 0.5\%$.

Optimization of the Detection Conditions and Standard Curve. The development of fluorescence intensities on the test and control lines can indirectly reflect the dynamic interaction between FNs-mAbs and ENR, FNs-mAbs and ENR-BSA, or the FNs-mAbs ENR and Abs on the sensor. To our knowledge, this is the first kinetic description behind the antibody–antigen interaction using a FNs label and the matrix effects for the quantitative ICTS sensor detection of ENR in chicken meat samples. The results shown in Figure 3A indicated that, after addition of the blank (0.01 M PB buffer, pH 7.0), the slopes between the kinetic curves for the test line and the control line exhibited a significant difference in the first 20-min of the assay but appeared almost the same in the last 20-min of a 40-min total assay time. The FI_T/FI_C ratio reached a constant in the last 20-min of monitoring showing the same slope between the two kinetic curves. Moreover, the FI_T/FI_C ratio reached a constant after the first 10–20 min in the presence of higher ENR concentration, Figure 3B. Thus, signals for quantitative analysis were measured at 20 min after the sample addition in all the succeeding studies.

The FI_T/FI_C ratio can eliminate the strip to strip effects in the immunoassay detection of ENR as well as shorten the strip interpretation time. Meanwhile, the ionic strength and pH variation in the immunoreaction system could significantly influence the binding efficiency of antigen and antibody by changing the activity of antigen-combining site of antibody

molecules.^{32–35} To evaluate the effect of ionic strength on the strip sensitivity, the 0.01 M PB (pH 7.0) was modified to contain 0, 0.1, 0.2, 0.4, 0.5, 0.6, and 0.7 M NaCl that was used as the strip running buffer. The results shown in Figure 3C indicated that the FI_T value was dependent on the ionic strength. At NaCl concentration from 0 to 0.2 mol/L the FI_T was reduced from 1314 ± 49 to 1076 ± 33 but the signal increased to 1737 ± 48 until it reached a constant at 1806 ± 63 when the NaCl concentration was increased from 0.6 to 0.7 mol/L. The FI_T/FI_C ratio also increased from 0.85 ± 0.06 to a constant between 1.98 ± 0.07 to 2.02 ± 0.06 ($P < 0.01$, $n = 3$) at the higher NaCl concentrations. In addition, the inhibition rate (B/B_0) of the strip for the 1 ng/mL ENR spiked concentration was increased significantly from $54.3\% \pm 3.5\%$ (0 M NaCl, $n = 3$) to $75.9\% \pm 3.3\%$ (0.6 M NaCl, $n = 3$, $p < 0.01$). These results indicated that higher sensor sensitivities were obtained at higher salt concentration with the best signal and inhibition ration being displayed at 0.6 M NaCl.

The effect of pH on the antibody–antigen interaction kinetics was evaluated by running the assay using 0.01 M PB buffer containing 0.6 M NaCl with pH in the range of 4–9. The results in Figure 3D showed that FI_T kept a relatively constant value at a pH range of 4–7, whereas it showed a significant decline from 1914 ± 71 (pH 7.0) to 1141 ± 51 (pH = 9) as the pH value changed from 7 to 9. The FI_T/FI_C ratio variation kept a similar trend, which exhibited a relatively constant value of 2.03 ± 0.01 , 1.97 ± 0.01 , 1.96 ± 0.01 , and 2.02 ± 0.01 ($P > 0.05$, $n = 3$) when the pH was changed from 4.0 to 7.0, and the FI_T/FI_C ratio declined to 1.09 ± 0.01 when the pH shifted to 9.0. These results showed that samples with stronger ionic strength and lower pH improved the FI_T on the test line

resulting in a higher sensitivity. In acid aqueous solution, ENR is more inclined to maintain the undissociated state. A high salt concentration can improve the ENR solubility in acid condition to enhance recognition ability of anti-ENR antibody to ENR molecules. Using these results, a 0.01 M PB containing 0.6 M NaCl at a pH 7.0 buffer was used for all subsequent detections.

To investigate whether the strip could provide quantitative detection of ENR in chicken meat, the calibration curve was determined by running twelve (12) ENR standard solutions on the FNs ICTS. The chicken meat contains a lot of fat, protein, and other materials, which could interfere with the color development of both the test line and control line. To decrease the interference from these components in matrices, the standard ENR solutions were prepared by diluting the ENR stock solution in chicken extract to a final concentration of 0 (as negative control), 0.01, 0.025, 0.05, 0.1, 0.3, 0.5, 0.8, 1.0, 2.0, 3.0, or 3.5 ng/mL, respectively. The FI_T/FI_C ratio between the negative control and positive samples were designated B_0 and B , respectively. Figure 4 shows the logarithmic calibration curve of

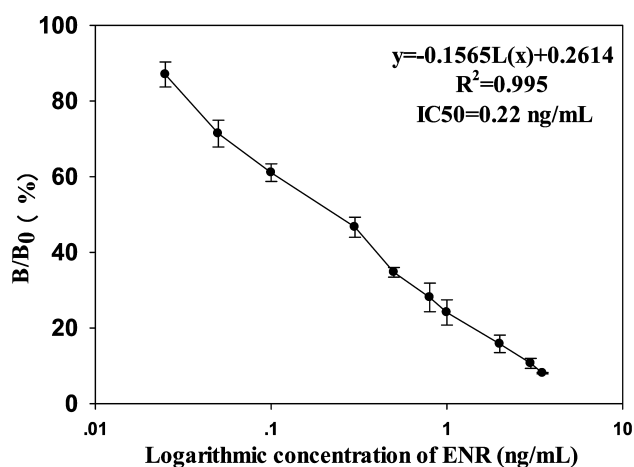


Figure 4. Calibration curves for ENR quantitative analysis (signals expressed as B/B_0 (%), where B and B_0 are the signals obtained with ENR-spiked samples and negative sample at 0 to 3.5 ng/mL ($n = 5$). The linear range of detection in chicken extract was established at 0.025 to 3.500 ng/mL. The upper limit of measurable concentration was 3.500 ng/mL. The limit of detection (LOD) was calculated at 0.02 ng/mL in chicken extract.

the B/B_0 ratios against ENR concentrations. Error bars were based on three duplicate measurements at different concentrations. The data exhibited a linear range between 0.025 and 3.500 ng/mL with a half maximal inhibitory concentration (IC_{50}) at 0.22 ± 0.02 ng/mL ($n = 3$). The regression equation was $y = -0.1565 \log(x) + 0.2614$ ($0.025 \leq x \leq 3.5$ ng/mL) where y is % B/B_0 and x is the ENR concentration, with a reliable correlation coefficient of $R^2 = 0.995$.

Assay Validation. The applicability of the FNs ICTS was validated in fifty (50) spiked raw chicken samples. The results showed a limit of detection (LOD) calculated at 0.02 ng/mL in chicken extract, which is equivalent to $0.12 \mu\text{g/kg}$ in chicken meat (resulting from a six folds dilution factor during extraction), respectively, according to the mean plus 3-fold standard deviation of the determined concentrations of twenty (20) randomly chosen negative chicken meat samples.^{10,36,37}

The precision of the intra- (within a day) and inter-assay (between 3 consecutive days at 3 assays each day) variations was used to evaluate the accuracy of the strip. Three spiked

chicken extracts, covering low, medium, and high levels of ENR concentrations, were prepared for intra- and inter-assay precision analysis (Table 1). Intra-assay was accomplished

Table 1. Precision of the FNs ICTS

sample (mg/mL)	intra-assay precision			inter-assay precision ^b		
	mean ^a (mg/mL)	SD (mg/mL)	CV (%)	mean (mg/mL)	SD (mg/mL)	CV (%)
0.5	0.55	0.03	6.04	0.54	0.07	12.96
1.0	0.98	0.07	6.92	1.03	0.13	12.61
2.0	1.83	0.12	6.66	2.02	0.24	11.88

^aMean value of 6 replicates. ^binter-assay was completed for 3 days in a row, three times per day, with 6 replicates at each concentration.

with 6 replicates at each concentration while inter-assay was completed for 3 consecutive days at three times per day with 6 replicates at each concentration. The results shown in Table 1 indicated that the intra- and inter-assay coefficient of variations (CVs) were 6.04% and 12.96% at 0.5 ng/mL, 6.92% and 12.61% at 1.0 ng/mL, and 6.66% and 11.88% at 2.0 ng/mL ENR, respectively. These intra- and inter-assay variations are acceptable levels of precision for ENR strip quantification.^{38–40}

Comparison between Strip and a Commercial Immunoassay ELISA Kit. To evaluate the acceptability of the new FNs ICTS sensor for ENR, a comparative study with a widely accepted ELISA kit method on fifty independent chicken meat samples bought from surrounding food markets was performed. The results in Figure 5A showed a highly significant correlation ($R^2 = 0.97$, $p < 0.01$) between the concentrations of ENR generated by the two assays. The slope of the resultant linear regression line was equal to 0.91. The FNs ICTS sensor for ENR exhibited a slightly better recovery range for ENR on the fifty (50) positive samples at 78.54% to 118.63%, while those of the ELISA kit were 64–120% (Figure 5B). These results are not significantly different ($p > 0.05$) considering that the FNs ICTS assay took only 20 min to complete while the ELISA kit took 90 min. Thus, these results suggested that the new FNs ICTS sensor was comparable and even slightly better in recovery for ENR than the commercial ELISA kit.

CONCLUSIONS

In summary, we successfully developed a sensitive, rapid, low cost, and user-friendly FNs ICTS quantitative sensor, using $\text{Ru}(\text{phen})_3^{2+}$ -doped silica nanoparticles as fluorescent reporters to screen ENR residues in chicken meat samples. To make the ENR biosensor useable for on-site monitoring, a portable fluorescence strip reader that was previously assembled in our lab was used. The portable reader was equipped with a software called the “watchdog” that was designed to calculate the ENR concentration from the samples. The signals from the FNs ICTS sensor that were recorded with the portable reader were reported as FI_T/FI_C ratio to effectively eliminate signal variations from strip to strip, sample variability, and matrix interferences. Using the optimized parameters, the LOD of the FNs ICTS sensor for ENR was established at 0.02 ng/mL in chicken extract that is equivalent to $0.12 \mu\text{g/kg}$ in the chicken meat samples. The intra- and inter-assay coefficient of variations (CVs) were as low as 6.04% and as high as 12.96%, which is acceptable for immunoassays. Furthermore, the FNs ICTS sensor reliability for ENR sensing was comparable to an existing commercially available ELISA kit.

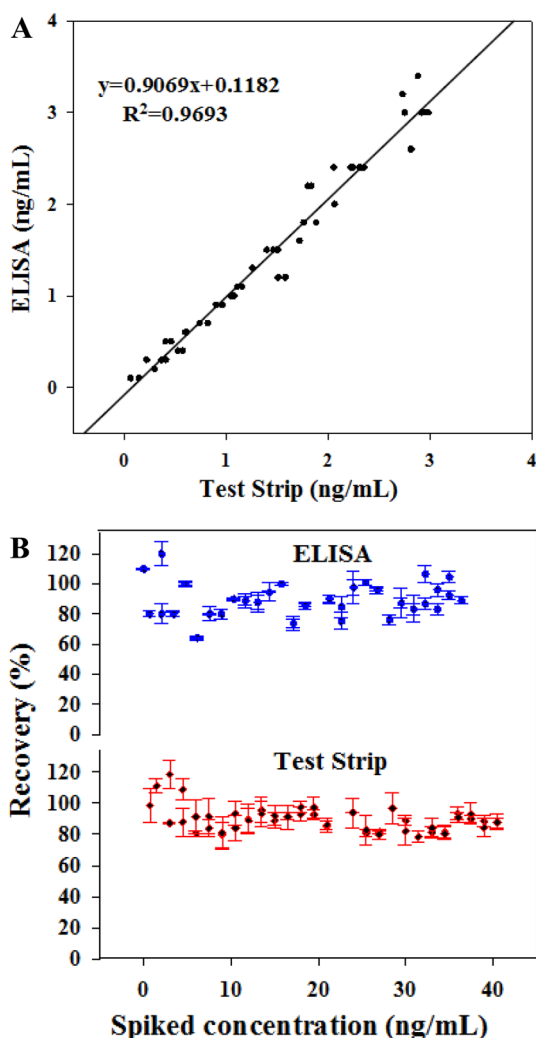


Figure 5. Comparative study between a FNs ICTS sensor and a commercially available ELISA kit in 50 spiked chicken meat samples with ENR concentrations from 0.0625 to 3.375 ng/mL. Correlation analysis of the detectable concentration between the two methods (A) and recovery of the two methods in different spiked ENR concentrations (B). Recovery stands for the ratio, which can be calculated from the value of actual detection ENR concentration (AC) and the value of actual spiked ENR concentrations (SC), recovery (%) = $AC/SC \times 100$.

The new FNs ICTS sensor took only 20 min to perform using small sample volume at 80 μ L and it is anticipated that even lower sample volumes may be usable with further optimization. In addition, the portable reader for the sensor allowed the assay performance on site with easy and fast release of results because of the built in “watchdog”. The FNs ICTS sensor holds promise for on-site detection of ENR and other chemicals or biochemicals in food samples.

■ ASSOCIATED CONTENT

● Supporting Information

Additional material as described in the text. This material is available free of charge via the Internet at <http://pubs.acs.org>.

■ AUTHOR INFORMATION

Corresponding Author

*Address: State Key Laboratory of Food Science and Technology and Jiangxi-OAI Joint Research Institute, Nan-

chang University, 235 Nanjing East Road, Nanchang 330047, P. R. China (Y.X.); State Key Laboratory of Food Science and Technology, Nanchang University, 235 Nanjing East Road, Nanchang 330047, P. R. China (H.X.). Phone: +0086-791-8833-4578 (Y.X.); +0086-791-8830-4447, ext 9512 (H.X.). Fax: +0086-791-8833-3708 (Y.X.); +0086-791-8830-4400 (H.X.). E-mail: yhxiongchen@163.com (Y.X.); kidyxu@163.com, HengyiXu@ncu.edu.cn (H.X.).

Author Contributions

[#]These authors contributed equally to this work.

Notes

The authors declare no competing financial interest.

■ ACKNOWLEDGMENTS

This work was supported by a grant from the National Basic Research Program of China (2013CB127804) and “Twelfth Five-Year Plan” for National Science and Technology Support Program (2012BAK17B02 and 2011BAK10B04), Natural Science Foundation of Jiangxi Province, China (No. 2010GZN0143 and 20114BAB214017), and a grant from the Research Foundation for Young Scientists of State Key Laboratory of Food Science and Technology, Nanchang University, China (No. SKLF-QN-201115).

■ REFERENCES

- (1) Filigenzi, M. S.; Ehrke, N.; Aston, L. S.; Poppenga, R. H. *Food Addit. Contam., Part A* **2011**, 28, 1324–1339.
- (2) Khot, L. R.; Panigrahi, S.; Lin, D. *Sens. Actuators, B* **2011**, 153, 1–10.
- (3) Liu, G.; Chen, H.; Peng, H.; Song, S.; Gao, J.; Lu, J.; Ding, M.; Li, L.; Ren, S.; Zou, Z.; Fan, C. *Biosens. Bioelectron.* **2011**, 28, 308–313.
- (4) Sankaran, S.; Panigrahi, S.; Mallik, S. *Biosens. Bioelectron.* **2011**, 26, 3103–3109.
- (5) Li, Z.; Wang, Y.; Kong, W.; Li, C.; Wang, Z.; Fu, Z. *Biosens. Bioelectron.* **2013**, 39, 311–314.
- (6) Tang, D.; Saucedo, J. C.; Lin, Z.; Ott, S.; Basova, E.; Goryacheva, I.; Biselli, S.; Lin, J.; Niessner, R.; Knopp, D. *Biosens. Bioelectron.* **2009**, 25, 514–518.
- (7) Li, H.; Wei, Q.; He, J.; Li, T.; Zhao, Y.; Cai, Y.; Du, B.; Qian, Z.; Yang, M. *Biosens. Bioelectron.* **2011**, 26, 3590–3595.
- (8) Tang, J.; Tang, D.; Su, B.; Huang, J.; Qiu, B.; Chen, G. *Biosens. Bioelectron.* **2011**, 26, 3219–3226.
- (9) Moreno-Guzman, M.; Ojeda, I.; Villalonga, R.; Gonzalez-Cortes, A.; Yanez-Sedeno, P.; Pingarron, J. M. *Biosens. Bioelectron.* **2012**, 35, 82–86.
- (10) Oh, S. W.; Kim, Y. M.; Kim, H. J.; Kim, S. J.; Cho, J. S.; Choi, E. *Y. Clin. Chim. Acta* **2009**, 406, 18–22.
- (11) Hong, W.; Huang, L.; Wang, H.; Qu, J.; Guo, Z.; Xie, C.; Zhu, Z.; Zhang, Y.; Du, Z.; Yan, Y.; Zheng, Y.; Huang, H.; Yang, R.; Zhou, L. *J. Microbiol. Methods* **2010**, 83 (2), 133–140.
- (12) Qu, Q.; Zhu, Z.; Wang, Y.; Zhong, Z.; Zhao, J.; Qiao, F.; Du, X.; Wang, Z.; Yang, R.; Huang, L.; Yu, Y.; Zhou, L. *J. Microbiol. Methods* **2009**, 79, 121–123.
- (13) Yan, Z.; Zhou, L.; Zhao, Y.; Wang, J.; Huang, L.; Hu, K.; Liu, H.; Wang, H.; Guo, Z.; Song, Y.; Huang, H.; Yang, R. *Sens. Actuators, B* **2006**, 119, 656–663.
- (14) Yang, Q.; Gong, X.; Song, T.; Yang, J.; Zhu, S.; Li, Y.; Cui, Y.; Zhang, B.; Chang, J. *Biosens. Bioelectron.* **2011**, 30, 145–150.
- (15) Zou, Z.; Du, D.; Wang, J.; N. Smith, J.; Timchalk, C.; Li, Y.; Lin, Y. *Anal. Chem.* **2010**, 82, 5125–5133.
- (16) Xia, X.; Xu, Y.; Zhao, X.; Li, Q. *Clin. Chem.* **2009**, 55, 179–182.
- (17) Xu, Y.; Li, Q. *Clin. Chem.* **2007**, 53, 1503–1510.
- (18) Pyo, D.; Yoo, J. *J. Immunoassay Immunochem.* **2012**, 33, 203–222.

- (19) Ruggi, A.; Beekman, C.; Wasserberg, D.; Subramaniam, V.; Reinhoudt, D.; van Leeuwen, F. W. B.; Velders, A. H. *Chem.—Eur. J.* **2011**, *17*, 464–467.
- (20) Rossi, L. M.; Shi, L.; Rosenzweig, N.; Rosenzweig, Z. *Biosens. Bioelectron.* **2006**, *21*, 1900–1906.
- (21) Lian, W.; Litherland, S. A.; Badrane, H.; Tan, W.; Wu, D.; Baker, H. V.; Gulig, P. A.; Lim, D. V.; Jin, S. *Anal. Biochem.* **2004**, *334*, 135–144.
- (22) Zhang, D.; Wu, Z.; Xu, J.; Liang, J.; Li, J.; Yang, W. *Langmuir* **2010**, *26*, 6657–6662.
- (23) Shim, J. H.; Shen, J. Y.; Kim, M. R.; Lee, C. J.; Kim, I. S. *J. Agric. Food. Chem.* **2003**, *51*, 7528–7532.
- (24) Zhang, H. T.; Jiang, J. Q.; Wang, Z. L.; Chang, X. Y.; Liu, X. Y.; Wang, S. H.; Zhao, K.; Chen, J. S. *J. Zhejiang Univ. Sci., B* **2011**, *12*, 884–891.
- (25) Chen, X.; Xu, H.; Lai, W.; Chen, Y.; Yang, X.; Xiong, Y. *Food Addit. Contam., A* **2012**, *29*, 383–391.
- (26) Wang, L.; Wu, X.; Xie, Z. *J. Sep. Sci.* **2005**, *28*, 1143–1148.
- (27) Chen, J.; Xu, F.; Jiang, H.; Hou, Y.; Rao, Q.; Guo, P.; Ding, S. *Food Chem.* **2009**, *113*, 1197–1201.
- (28) Yu, F.; Wu, Y.; Yu, S.; Zhang, H.; Qu, L.; Harrington Pde, B. *Spectrochim. Acta, Part A* **2012**, *93*, 164–168.
- (29) Zhao, Y.; Zhang, G.; Liu, Q.; Teng, M.; Yang, J.; Wang, J. *J. Agric. Food. Chem.* **2008**, *56*, 12138–12142.
- (30) Zou, M.; Gao, H.; Li, J.; Xu, F.; Wang, L.; Jiang, J. *Anal. Biochem.* **2008**, *374*, 318–324.
- (31) Pretsch, E.; Seibl, J.; Simon, W.; Clerc, T. *Tables of Spectral Data for Structure Determination of Organic Compounds*, 2nd ed.; Springer-Verlag: New York, 1983.
- (32) Lu, Z. R.; Kopečková, P.; Kopeček, J. *Macromol. Biosci.* **2003**, *3*, 296–300.
- (33) Hianik, T.; Ostatná, V.; Sonlajtnerova, M.; Grman, I. *Bioelectrochemistry* **2007**, *70*, 127–133.
- (34) Pei, Z.; Anderson, H.; Myrskog, A.; Dunér, G.; Ingemarsson, B.; Aastrup, T. *Anal. Biochem.* **2010**, *398*, 161–168.
- (35) Zhao, X.; Pan, F.; Garcia-Gancedo, L.; J. Flewitt, A.; M. Ashley, G.; Luo, J.; R. Lu, J. *J. R. Soc. Interface* **2012**, *9*, 2457–2467.
- (36) Ahn, J. S.; Choi, S.; Jang, S. H.; Chang, H. J.; Kim, J. H.; Nahm, K. B.; Oh, S. W.; Choi, E. Y. *Clin. Chim. Acta* **2003**, *332*, 51–59.
- (37) Pleadin, J.; Vulić, A.; Perši, N.; Vahčić, N. *Meat Sci.* **2010**, *86*, 733–737.
- (38) Bai, Y.; Liu, Z.; Bi, Y.; Wang, X.; Jin, Y.; Sun, L.; Wang, H.; Zhang, C.; Xu, S. *J. Agric. Food Chem.* **2012**, *60*, 11618–11624.
- (39) Semenova, V. A.; Schiffer, J.; Steward-Clark, E.; Soroka, S.; Schmidt, D. S.; Brawner, M. M.; Lyde, F.; Thompson, R.; Brown, N.; Foster, L.; Fox, S.; Patel, N.; Freeman, A. E.; Quinn, C. P. *J. Immunol. Methods* **2012**, *376*, 97–107.
- (40) Food and Drug Administration Guidance for Industry: Bioanalytical Method Validation, 2001. <http://www.fda.gov/downloads/Drugs/GuidanceComplianceRegulatoryInformation/Guidances/ucm070107.pdf>.